A molecular dynamics study of a fullerene-cyanoadamantane mixture

2002 J. Phys.: Condens. Matter 14 1223

(http://iopscience.iop.org/0953-8984/14/6/309)

INSTITUTE OF PHYSICS PUBLISHING JOURNAL OF PHYSICS: CONDENSED MATTER

J. Phys.: Condens. Matter **14** (2002) 1223–1230 PII: S0953-8984(02)26239-6

A molecular dynamics study of a fullerene–cyanoadamantane mixture

S Pałucha, K Kaczor and Z Gburski

Institute of Physics, Uniwersytecka 4, Katowice, 40-00, Poland

E-mail: palucha@us.edu.pl, kaczor@us.edu.pl and zgburski@us.edu.pl

Received 27 June 2001, in final form 27 November 2001
Published 1 February 2002
Online at stacks.iop.org/JPhysCM/14/1223

Abstract

We use a molecular dynamics method to simulate the relaxation processes of cyanoadamantane molecules in a fullerene environment, for two densities and several temperatures (over the range 400–2000 K). The interactions between the C_{60} molecules were modelled using the approach proposed by Girifalco. Cyanoadamantane molecules were represented by a rigid three-site model. The dynamics of molecules in the system have been studied by inspecting the plots of the translational $C_v(t)$ and angular $C_\omega(t)$ velocity autocorrelation functions, their Fourier transforms, and the temperature dependences of the corresponding diffusion coefficients. We have found two kinds of rotational dynamics of the cyanoadamantane molecule in the solid phase of the mixture studied.

1. Introduction

Fullerene C_{60} molecules at low temperature form a face-centred-cubic (fcc) structured solid. For each fullerene molecule in such a matrix, there are three available sites where other atoms can go. The study of gases permeating solid fullerite [1–3] aims at understanding the effect which doping molecules exert on the host matrix. Very recently researchers have shown growing interest in studying the fullerites doped by relatively large molecules [4]. This is connected with the appearance of the high-temperature superconductivity when the jostling of guest molecules increases the lattice spacing between fullerenes. In [5] we investigated the diffusion of small dipolar molecules (nitrogen oxide) inside a C_{60} fullerite matrix. It would be of interest to study such processes with larger molecules of impurities with stronger dipole moments, which can reveal more significant effects of impurities on the fullerine matrix and vice versa.

The molecule which possess the feature mentioned and is currently the subject of many studies is cyanoadamantane ($C_{10}H_{15}CN$) denoted here as CNadm. The cyano group (CN) is responsible for the molecule's high dipole moment ($\mu = -3.92$ D), which causes the bulk cyanoadamantane sample to show interesting phases, including the plastic one. With the onset

Table 1. Simulation parameters.

ij	ε_{ij} (kJ mol^{-1})	σ_{ij} (Å)
N–N	0.7099	3.25
C–C	0.3089	3.55
N–C	0.4683	3.40
N-adm	2.4290	4.70
C-adm	1.6020	4.90
adm–adm	8.3110	6.30

of cooling CNadm begins to evolve from the fluid phase, which is mainly characterized by translational motion, then the plastic, glassy and crystalline states appear [6–8]. The plastic phase is stable from its melting point at $T_m \approx 445$ K, down to $T_t \approx 238$ K [9]. This structure is characterized by the orientational disorder of molecules and translational order of molecular centres of mass ($Fm3m$ crystalline structure). The rotator phase can be quenched by supercooling to the glassy crystal state. In this state the molecular orientations are frozen, which causes extremely large reorientational relaxation times.

Here we focus on the dynamics of CNadm molecules treated as guests inside the fullerite matrix.

2. Simulation procedure

It is well established that the interaction between two C_{60} molecules can be well described in terms of the overall potential proposed by Girifalco [10], with the interaction values α and β equal to, respectively, 4.4775 and 0.0081 kJ mol^{-1} (the meaning of the α and β coefficients is the same as in [10]).

The interactions between two CNadm molecules were simulated with the help of the simple cyanoadamantane model [11]. It is well known that adamantane molecule has a fairly spherical shape and the anisotropy of CNadm comes from the presence of the CN group. One can represent this by a rigid, three-site model, instead of the full model with 27 atoms, as proposed by Cathiaux [11]. The first and second sites correspond to nitrogen and carbon atoms while the last one corresponds to the whole adamantane group. The interactions between the site atoms and the supersite (adm) have been modelled in terms of the Lennard-Jones potentials representing i–j interactions between sites belonging to different molecules. In this case we have

$$V_{ij}(r) = 4\varepsilon_{ij}\left[\left(\frac{\sigma_{ij}}{r}\right)^m - \left(\frac{\sigma_{ij}}{r}\right)^n\right] \tag{1}$$

with ε_{ij} and σ_{ij} given in table 1. In all cases, the values of n and m are 6 and 12 respectively. However, the parameters for the adm–adm interaction have special values of n and m, namely, 10 and 16 [11, 12]. The values of interaction energy parameter $\varepsilon_{\mathrm{adm-adm}}$ and their minimum distance $\sigma_{\mathrm{adm-adm}}$ are also given in table 1 (taken from [11, 12]).

Similarly to the interaction between two fullerenes, the interaction between the C_{60} and CNadm molecules can be taken into account by integrating over the C_{60} sphere the L–J interaction between a single atomic (carbon) member of the C_{60} molecule and a particular site atom of CNadm. The integration of the latter over the entire fullerene sphere results in the following C_{60}–site overall potential [13]:

$$V_{C_{60}\text{-site}}(s) = 60\left(\frac{c_6}{R^6}F_6(s) + \frac{c_{12}}{R^{12}}F_{12}(s)\right) \tag{2}$$

where $2R = \sigma_{C_{60}}$, $c_6 = -4\varepsilon_{\text{C-site}}\sigma^6_{\text{C-site}}$ and $c_{12} = 4\varepsilon_{\text{C-site}}\sigma^{12}_{\text{C-site}}$, where $\varepsilon_{\text{C-site}}$ and $\sigma_{\text{C-site}}$ are given in table 1. Then $F_n = \frac{1}{s(n-2)}[(1-2s)^{2-n} - (1+2s)^{2-n}]$.

To obtain a more realistic model, in addition to the van der Waals and repulsive interactions, one has to also take into account the electrostatic interaction between CNadm molecules, i.e. one has to add two charges with value 0.712 e, negative on the nitrogen atom and positive on the carbon atom.

We have applied the above model to carry out a series of computer simulations in the constant temperature ensemble (NVT), with a fixed number, N , of particles and molar volume V. We have performed our simulation for two densities, $\rho_{\text{I}} = 1.031$ g cm^{-3} (250 fullerenes mixed with 250 CNadm molecules) and $\rho_{\text{II}} = 0.874$ g cm^{-3}(250 fullerenes mixed with 304 CNadm). The C_{60} and CNadm molecules were initially placed on two interpenetrating lattices in order to obtain a single fcc structure. The lattice spacings of the starting configuration were chosen to be equal to that of crystalline C_{60} at room temperature, e.g. 14.138 Å [14]. Our simulations covered the temperature range 400–2000 K.

The integration algorithm timestep was 5 fs. Prior to the actual data collection the system was equilibrated for at least 10^4 timesteps during which velocity scaling was applied. The production runs consisted of around 10^5 steps. We used the Ewald summation method for long-range electrostatic interaction. The potential cutoff radius was equal to the half of the simulation box.

3. Discussion and results

The reorientation of a single CNadm molecule and their global collective motion can be monitored in terms of $C_u(t) = \langle \boldsymbol{u}(t) \cdot \boldsymbol{u}(0)\rangle \cdot \langle \boldsymbol{u}(0) \cdot \boldsymbol{u}(0)\rangle^{-1}$, where $\boldsymbol{u}$ denotes a unit vector along the molecular axis, and $C_M(t) = \langle \boldsymbol{M}(t) \cdot \boldsymbol{M}(0)\rangle \cdot \langle \boldsymbol{M}(0) \cdot \boldsymbol{M}(0)\rangle^{-1}$ with the global orientation $\boldsymbol{M}(t) = \sum_{i=1}^{n} \boldsymbol{u}_i(t)$, where n is the total number of CNadm particles.

In figure 1 we present $C_u(t)$ which gives the change of orientation for one molecule as a function of time. For higher density ρ_{I} (see figure 1(a)) at a lower temperature of 400 K one observes the slow reorientational relaxation of the CNadm molecules trapped inside the fullerite matrix. We see that there is a significant variation of $C_u(t)$ with temperature. An increase of temperature leads to a spectacularly faster decay of $C_u(t)$. Apparently at higher temperatures the CNadm molecules have much more rotational freedom. At $T = 1400$ K the caging effect is no longer strong enough to produce tumbling rotational diffusion, so one has an ensemble of almost free rotors. As one expects, for the sample of lower density ρ_{II} the caging effect is less effective. It is relatively strong at the lower temperature of $T = 400$ K, around $T = 1000$ K the adamantane molecules already rotate almost freely.

As one would expect, the increase of temperature leads to a faster decay of global collective motion, see $C_M(t)$ presented in figure 2. At the lower temperature, there are strong correlations between CNadm molecules. One can see that for the system with higher density (ρ_{I}) $C_M(t)$ becomes less correlated at 900 K than $C_u(t)$ at the same temperature. Namely, at 800 K, the translational diffusion of CNadm molecules starts and the global collective motion is disturbed by the fullerenes.

To get further insight into the molecular motion we calculated the velocity autocorrelation function $C_v(t) = \langle \boldsymbol{v}(t) \cdot \boldsymbol{v}(0)\rangle \cdot \langle \boldsymbol{v}(0) \cdot \boldsymbol{v}(0)\rangle^{-1}$ and the angular velocity autocorrelation function $C_\omega(t) = \langle \boldsymbol{\omega}(t) \cdot \boldsymbol{\omega}(0)\rangle \cdot \langle \boldsymbol{\omega}(0) \cdot \boldsymbol{\omega}(0)\rangle^{-1}$, as well as their frequency Fourier transforms (FT), for both C_{60} and CNadm molecules: see figures 3 and 4.

The main difference between the two densities was observed for 400 K. The correlation function $C_v(t)$ of C_{60} (figure 3(a)) for higher density (ρ_{I}) have a strong negative event with many bumps, whereas at lower density (ρ_{II}) one can only see a negative pronounced tail

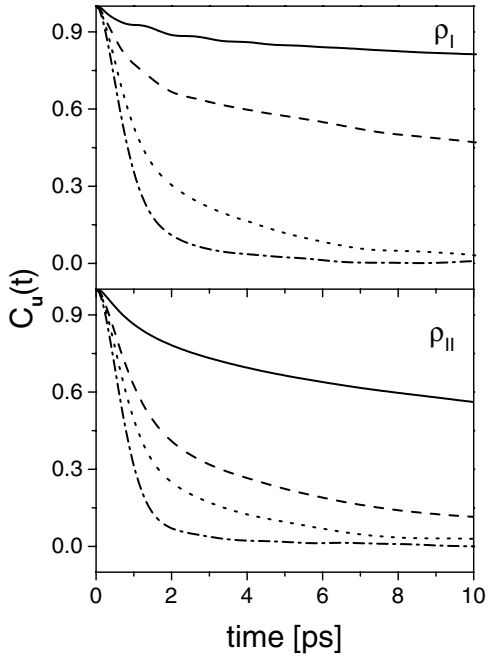

Figure 1. The time autocorrelation functions $C_u(t)$ at two densities ρ_{I} and ρ_{II}. Solid, dashed, dotted and dash-dotted curves indicate $T = 400$, 900, 1100 and 1400 K, respectively.

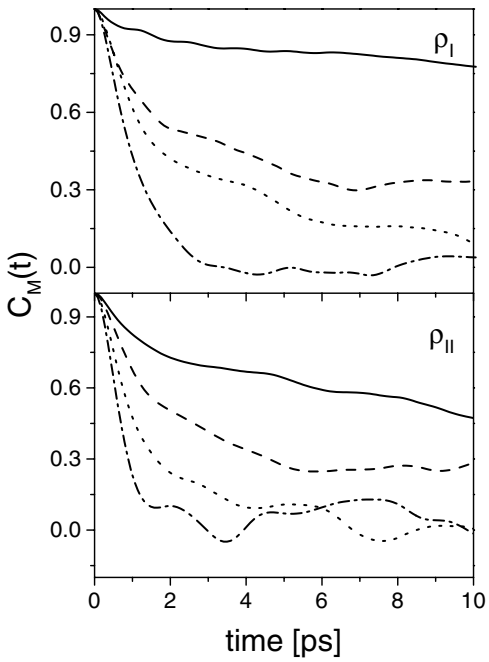

Figure 2. The time autocorrelation functions $C_M(t)$ at two densities ρ_{I} and ρ_{II}. Solid, dashed, dotted and dash-dotted curves indicate $T = 400$, 900, 1100 and 1400 K, respectively.

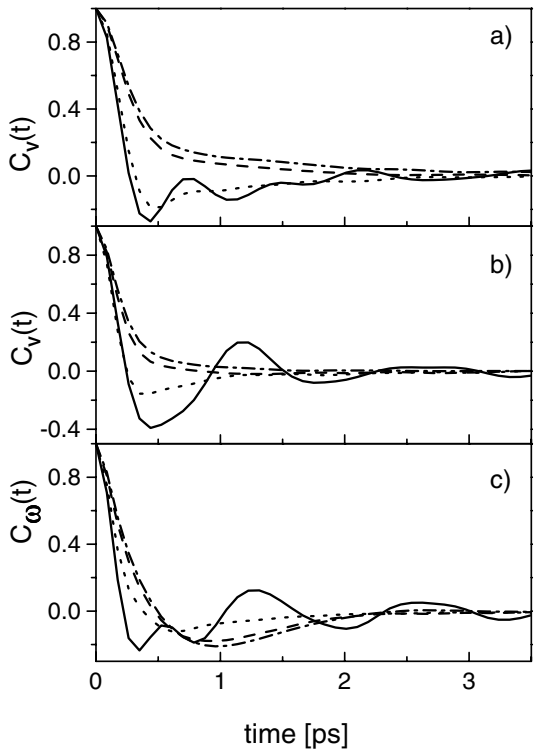

Figure 3. The time correlation functions; (a) $C_v(t)$ for the C_{60} molecule, (b) $C_v(t)$ and (c) $C_\omega(t)$ for the CNadm molecule. The solid and dashed curves indicate the ρ_{I} density for $T = 400$ and 1400 K, respectively. The dotted and dashed–dotted curves indicate the ρ_{II} density for $T = 400$ and 1400 K, respectively.

without any bumps. The corresponding FT(ω) of $C_v(t)$, which is shown in figure 4(a), has for higher density (ρ_{I}) at least two groups of peaks placed around 20 and 50 cm^{-1}. At lower density (ρ_{II}) only one very broad FT(ω) peak is observed. The zero-frequency values of the FT($\omega = 0$) at $T = 400$ K implies a lack of translational diffusion of the C_{60} molecules, since the translational diffusion coefficient $D_{\mathrm{tr}} = \int_0^\infty \langle \boldsymbol{v}(t) \cdot \boldsymbol{v}(0) \rangle \, \mathrm{d}t \approx \mathrm{FT}(\omega = 0)$ [15], which is presented in figures 5(a) and (d).

The velocity correlation function of CNadm at higher density (ρ_{I}) oscillates almost periodically (figure 3(b)). Looking at the corresponding FT(ω) (figure 4), we see quite sharp peak with the maximum around 25 cm^{-1}. This can be interpreted as an almost periodical rebounding of CNadm molecules inside the C_{60} matrix. At lower density (ρ_{II}) the cage is not that tight, the adamantane molecules have more space to move on, we observe nonoscillatory decay of $C_v(t)$ and a broad distribution of FT(ω) (figures 3 and 4).

The angular velocity correlation function $C_\omega(t)$ of cyanoadamantane pulsates at higher density (ρ_{I}), the corresponding FT has two peaks. The sharp one at 25 cm^{-1} and much broader one around 53 cm^{-1}. The first peak at 25 cm^{-1} should be again associated with the effect of rebounding of adamantane inside a rigid cage, especially if we take into account that the pronounced maximum of FT(ω) at the same frequency of 25 cm^{-1} also appears in the case of translational motion of CNadm (see figure 3(b)). The second broad peak of FT(ω) around 53 cm^{-1} corresponds to the adamantane rotational density of states peak found by Raman

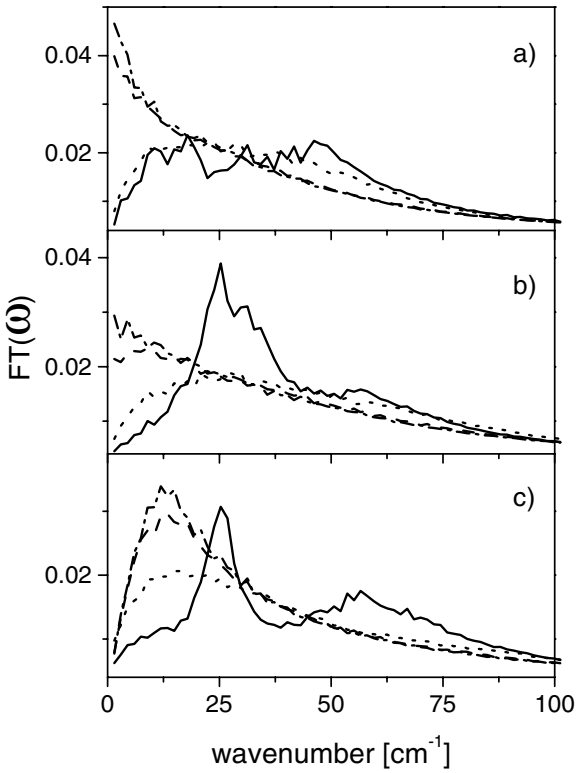

Figure 4. The FT of the time correlation functions: (a) FT-$C_v(t)$ for C_{60} molecules, (b) FT-$C_v(t)$ and (c) FT-$C_\omega(t)$ for CNadm molecules. Solid and dashed curves indicate the ρ_{I} density for $T = 400$ and 1400 K, respectively. Dotted and dashed–dotted curves indicate the ρ_{II} density for $T = 400$ and 1400 K, respectively.

spectroscopy [16] (50 cm^{-1}) and obtained also by Cathiaux *et al* during MD simulations of pure adamantane. At lower density (ρ_{II}) the motion of CNadm is less caged, the sharp peak associated with the rebounding disappears, we only observe a broad FT(ω) distribution with the fuzzy maximum around 16 cm^{-1}.

At a high temperature of $T = 1400$ K the translational velocity correlation functions of both fullerene and adamantane decay much more regularly, almost exponentially (see figures 3(a), (b))—this is known as the typical, fluid-like behaviour of $C_v(t)$ [17]. Additional support for this conclusion comes from the fact that at 1400 K the density dependence of $C_v(t)$ is much weaker compared to the low-temperature behaviour. We clearly see the vanishing of low-temperature oscillations of the $C_v(t)$ and FT(ω) peaks (around 25 cm^{-1}), this is connected with the disappearance of the caging effect—our system melts. Both fullerene and adamantane molecules can now translate since the translational diffusion coefficient $D_{\mathrm{tr}} \approx \mathrm{FT}(\omega = 0) \neq 0$ (figures 4(a), (b)). Looking at $C_\omega(t)$ of CNadm at $T = 1400$ K we see a rather regular decay (no oscillations) with a broad and shallow negative tail which is characteristic for the fluid phase. Only weak density dependence is observed in the fluid, in contrast to the low-temperature phase, where the influence of density on $C_\omega(t)$ is spectacular (see figure 3(c)). At $T = 400$ K, the decreasing density makes the cage less restrictive, the adamantane molecules rotate more freely but the translational motion remains frozen. However, at the higher temperature, $T = 1400$ K, the translational diffusion of both

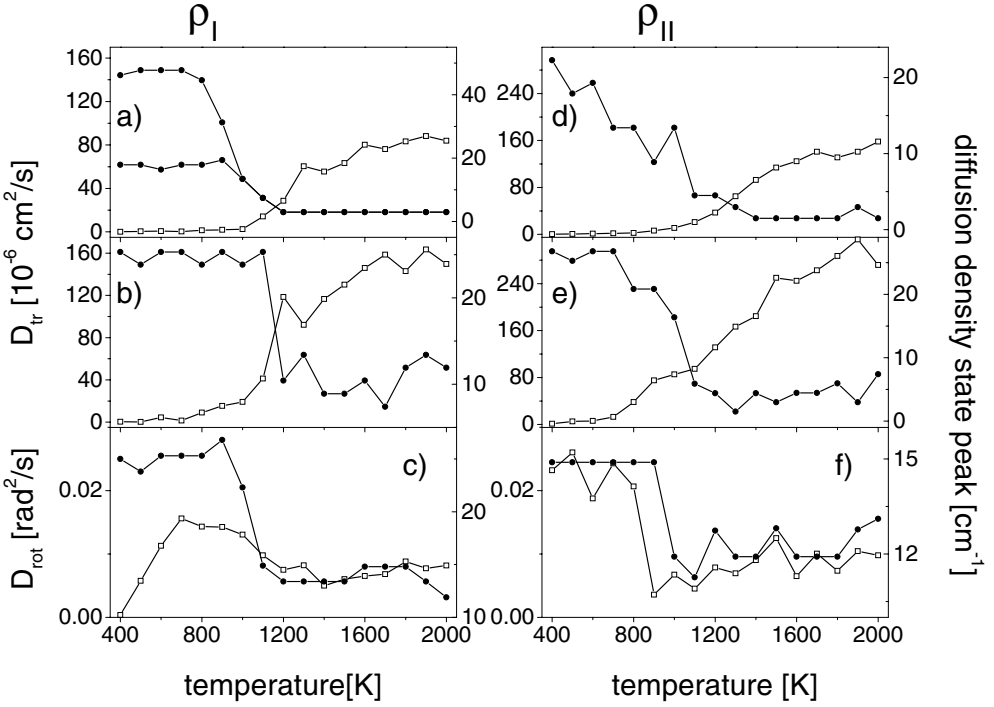

Figure 5. The temperature dependence of the diffusion coefficients (open squares) and diffusion density state peaks (filled circles) at two densities ρ_{I} ((a), (b) and (c)) and ρ_{II} ((d), (e) and (f)) obtained from $\mathrm{C}_v(t)$ of both C_{60} and CNadm, and from $\mathrm{C}_\omega(t)$ of CNadm.

fullerene and adamantane is active (see figure 5). In this case, a shift of the minimum of $\mathrm{C}_\omega(t)$ to middle times is observed, compared to the corresponding plot at low-temperature and low-density ρ_{II}. This can be connected with the fact that in the fluid phase the rotations are slaved to translations as the molecule must rotate in order to translate between the neighbouring ones.

So far we have discussed the overall correlation function plots, now we focus on the temperature dependence of the translational D_{tr} and rotational $D_{\mathrm{rot}} = \int_0^\infty \langle \omega(t) \cdot \omega(0) \rangle \, \mathrm{d}t$ diffusion coefficients. We also discuss how the first peaks of the FT of $\mathrm{C}_v(t)$ and $\mathrm{C}_\omega(t)$ (density states) evolve as a function of temperature (see figure 5).

At first, for higher density ρ_{I}, the translational diffusion of the C_{60} molecules starts at around 1000 K, grows quickly until 1300 K, then stabilizes. This is evidence for the phase transition (melting) of the fullerite host matrix at a temperature of about $T \approx 1200$ K (figure 5(a)). The weak diffusion of much lighter cyanoadamantanes begins earlier, at around 800 K, grows slowly until 1000 K (while the fullerite matrix is still rigid), then grows more quickly due to the realization of cage restrictions near the melting point, and then becomes stabilized in the fluid phase for $T > 1300$ K (figure 5(b)).

For the lower density ρ_{II} (figures 5(d) and (e)) the development of translational diffusion of both C_{60} and CNadm begins earlier (at about 700 K) and spreads widely up to 1500 K, consequently the melting of this solid mixture proceeds in a less dramatic way.

The rotational dynamics of CNadm at low temperature ($T < 800$ K) is quite different for two densities. The heating of the system activates the rotations ($D_{\mathrm{rot}}(T)$ increases) in the height density sample ρ_{I} which we have already associated—by inspecting the $\mathrm{C}_\omega(t)$ plots, see figure 3(c)—with the rotational libration of CNadm in a tight, rigid cage formed by fullerenes.

In contrast, in the same temperature region, $T < 800$ K, $D_{\mathrm{rot}}(T)$ systematically decreases for low-density ρ_{II}. Therefore, for $T < 800$ K, we can distinguish two rotational phases, depending on density. First, at higher density ρ_{I} the adamantane molecules can only perform quasi-periodical rotational librations (strong caging effect). To our knowledge the existence of this phase has not been reported so far in the case of the cyanoadamantane/fullerene mixture. Second, at ρ_{II} the cyanoadamantanes still cannot translate ($D_{\mathrm{tr}} \cong 0$), however they are able to reorientate more freely and this phase is often called 'plastic' [6, 9]. For the detailed characteristics, significance and applications of the crystalline plastic phase, see [18, 19] and references therein.

4. Conclusions

Using an MD technique we have studied the dynamics of molecules in a C_{60}–CNadm mixture. The various autocorrelation functions can be used to distinguish the difference between the solid, plastic and fluid phases. A finer analysis of the caging effect and the behaviour of the translational and rotational relaxations show that the appearance of various phases strongly depends on their densities. At low temperatures ($T < 800$ K) the librational and plastic phases appear, corresponding to high or low density, respectively. At high temperatures ($T > 1100$ K) the fluid phase occurs for both densities with the active translations and rotations, and the strong translational–rotational coupling.

Acknowledgments

This work was partly supported by the grant 2 PO3B 100 18 from the Polish Committee for Scientific Research (KBN). We thank the Wroclaw Center of Networking and Supercomputing for a generous allotment of IBM SP2 computer time.

References

[1] Cheng A and Klein M I 1992 *J. Chem. Soc. Faraday Trans.* **88** 1949
[2] Abramo M C and Caccamo C 1997 *J. Chem. Phys.* **106** 6475
[3] Pałucha S and Gburski Z 1999 *J. Mol. Struct.* **480** 343
[4] Schön J H, Kloc Ch and Batlogg B 2001 Published online August 30 10.1126/science 1 064 773 *(Science Express Reports)*
[5] Pałucha S, Dendzik Z and Gburski Z 2000 *J. Mol. Struct.* **555** 311
[6] Foulon M, Amoureux J P, Sauvajol J L, Cavrot J P and Muller M 1984 *J. Phys. C: Solid State Phys.* **17** 4213
[7] Amoureux J P, Decressain R, Sahour M and Cochon E 1992 *J. Physique* **2** 249
[8] Sauvajol J L, Bee M and Amoureux J P 1982 *Mol. Phys.* **46** 811
[9] Willart J F, Descamps M and Bezakour N 1996 *J. Chem. Phys.* **104** 2508
[10] Girifalco L A 1992 *J. Phys. Chem.* **95** 5370
[11] Cathiaux D, Sokolic F, Descamps M and Perera A 1999 *Mol. Phys.* **96** 1033
[12] Kuchta B, Descamps M and Affouard F 1998 *J. Chem. Phys.* **109** 6753
[13] Breton J, Gonzales-Platas J and Girardet C 1993 *J. Chem. Phys.* **99** 4036
[14] Lieber C H and Chen C C 1994 *Solid State Physics: Fullerenes* ed H Elrenreich and F Spaepen (San Diego: Academic)
[15] Allen M P and Tildesley D J 1987 *Computer Simulation of Liquids* (Oxford: Clarendon)
[16] Foulon M, Amoureux J P, Sauvajol J L, Lefebvre J and Descamps M 1983 *J. Phys. C: Solid State Phys.* **16** 265
[17] Hansen J P and McDonald I R 1986 *Theory of Simple Liquids* 2nd edn (London: Academic)
[18] Willart J F, Descamps M and van Miltenburg J C 2000 *J. Chem. Phys.* **112** 10 992
[19] Luty T, Rohleder K, Lefebvre J and Descamps M 2000 *Phys. Rev.* B **62** 8835